TITLE

Reactive Oxygen Detoxification Contributes to *Mycobacterium abscessus* Antibiotic Survival

AUTHORS

Nicholas A. Bates[1,2], Ronald Rodriguez[3,4], Rama Drwich[1], Abigail Ray[5], Sarah A. Stanley[3], Bennett H. Penn[1,6]*

AFFILIATIONS:

1. Department of Internal Medicine, University of California, Davis, California, USA
2. Graduate Group in Immunology, University of California, Davis, California, USA
3. Department of Molecular & Cell Biology, University of California, Berkeley, California, USA
4. Department of Plant & Microbial Biology, University of California, Berkeley, California, USA
5. Microbiology Graduate Group, University of California, Davis, California, USA
6. Department of Medical Microbiology and Immunology, University of California, Davis, California, USA

*Corresponding author

Email: bhpenn@ucdavis.edu

ABSTRACT

When a population of bacteria encounter a bactericidal antibiotic most cells die rapidly. However, a sub-population, known as “persister cells”, can survive for prolonged periods in a non-growing, but viable, state. Persister cell frequency is dramatically increased by stresses such as nutrient deprivation, but it is unclear what pathways are required to maintain viability, and how this process is regulated. To identify the genetic determinants of antibiotic persistence in mycobacteria, we

carried out transposon mutagenesis high-throughput sequencing (Tn-Seq) screens in *Mycobacterium abscessus* (*Mabs*). This analysis identified genes essential in both spontaneous and stress-induced persister cells, allowing the first genetic comparison of these states in mycobacteria, and unexpectedly identified multiple genes involved in the detoxification of reactive oxygen species (ROS). We found that endogenous ROS were generated following antibiotic exposure, and that the KatG catalase-peroxidase contributed to survival in both spontaneous and starvation-induced persisters. We also found that that hypoxia significantly impaired bacterial killing, and notably, in the absence of oxygen, KatG became dispensable. Thus, the lethality of some antibiotics is amplified by toxic ROS accumulation, and persister cells depend on detoxification systems to remain viable.

INTRODUCTION

A key goal of antibiotic therapy is the complete eradication of the pathogen. While many common infections respond rapidly to antibiotics, and high cure rates are achieved with 1-2 weeks of therapy[1,2], there are also infections where bacterial clearance is either very slow, or frequently incomplete. This challenge is exemplified by mycobacterial infections, where treatment courses extend from months to years to prevent relapse.

While the ability of mycobacteria to escape antibiotic-mediated killing is multifactorial, the phenomenon of antibiotic “persistence” is likely an important contributor[3-6]. Studies on penicillin dating from the 1940s noted that when a population of susceptible bacteria were exposed to a bactericidal antibiotic, the majority of the population died within a few hours, but that a small sub-population of ‘persisters’ remained viable for over a week[7]. Importantly, these persister cells had not acquired a mutation conferring heritable antibiotic resistance, and do not grow in the presence of the antibiotic. Rather, they have entered into a readily-reversable epigenetic state[8-10] where, despite antibiotic-mediated inhibition of critical processes, they are able to survive. Virtually all

bacterial species display the ability to form persister cells, and their development is strongly induced in response to stresses such as nutrient deprivation or acidic pH[6-7,11-12]. Notably, these same stresses are encountered in the lysosome of an activated immune cell[13], and studies of pathogens isolated from activated macrophages indeed show a strong immune-mediated increase in persister cells[5,14]. Thus, paradoxically, the immune system may actually impede bacterial eradication by antibiotics.

Persister formation has been studied extensively in model systems such as *Escherichia coli*, which has provided important insights, but also highlighted uncertainties of current models. Several different pathways have been implicated in *E. coli* persister formation, including the HipBA toxin-antitoxin system[15], guanosine pentaphosphate ((p)ppGpp) synthesis by RelA/SpoT enzymes[16,17], and Lon protease[16]. In each of these models, the postulated mechanism is to halt cell division and render the process targeted by antibiotics non-essential. However, important questions remain unanswered. It is unclear how persister cells remain viable when critical processes such as transcription or translation are arrested by antibiotics, as well as how the process is regulated and induced by stress.

Even the mechanism of cell death following antibiotic exposure itself remains uncertain, and somewhat controversial. Historically, antibiotics have been presumed to kill bacteria as a direct result of inhibition of their target molecule, such as β-lactam antibiotics disrupting cell wall integrity, directly leading to mechanical cell lysis[18]. However, a number of studies, largely from *E. coli*, have suggested that reactive oxygen species (ROS) accumulation triggered by antibiotic stress might also contribute to cell death[10,19-20]. Conversely, other studies have found no such association[21,22], leaving the role of ROS in antibiotic-mediated cell death unresolved.

Studying persister cell physiology in mycobacterial pathogens offers several advantages. Mycobacterial persister cells are particularly resilient, as *Mycobacterium smegmatis* (*Msmeg*) and *Mycobacterium tuberculosis (Mtb)* persisters can endure many weeks of antibiotic exposure[10,23-24]. Clinically, mycobacterial infections are difficult to eradicate. Fully-susceptible *Mtb* requires multiple antibiotics for four months or longer[25-26], whereas non-tuberculous mycobacteria typically require treatment for 12-18 months and have a relapse rates of roughly 50%[27]. *Mycobacterium abscessus* (*Mabs*) is among the most difficult of all bacterial pathogens to treat, because in addition to the possibility of forming persister cells, it is intrinsically resistant to many classes of antibiotics, leaving few treatment options[28]. This leads to the use of antibiotics with greater toxicity to patients, and a need to use these agents for prolonged periods to prevent relapse. Thus, identifying the genes that *Mabs* persister cells rely on for survival could be beneficial by highlighting pathways that might be targeted therapeutically to eliminate persister cells.

Previous genetic screens have studied antibiotic responses in mycobacteria, with some evaluating heritable resistance, and others investigating persister cell formation. Several studies of genetic resistance have successfully used either transposon mutagenesis with high-throughput sequencing of insertion sites (Tn-Seq) or CRISPR-based transcriptional repression with high-throughput sequencing of guide RNAs (CRISPRi) to identify genes promoting growth in sub-inhibitory concentrations of antibiotic. These studies have provided insights such as the importance of cell membrane permeability controlling antibiotic penetration into the cytoplasm[29-31]. Persister cell formation has proven challenging to study, likely because their low frequency leads to population bottlenecks that confound genetic analysis. Although screens in *Mtb* have been conducted in macrophages and mice, and genes such as *glpK* and *cinA* identified, overall the number of mutants isolated in these screens has been low[32-34]. There has been one highly-effective in vitro Tn-Seq study of rifampin survival in *Mtb* that isolated over 100 mutants[19], demonstrating the feasibility of genetic screening in this context. However, whether these

104 phenotypes seen with rifampin in *Mtb* extend to other organisms and other antibiotics remains to
105 be determined.
106
107 Here, we study persister cell formation in *Mabs*, and describe the results of genome-wide Tn-seq
108 screens seeking to identify the genes required for both spontaneous and starvation-induced
109 antibiotic persistence. We identified diverse pathways contributing to persister cell survival, and
110 unexpectedly, observed a prominent role for ROS detoxifying factors such as the catalase-
111 peroxidase enzyme KatG, which contributed to both spontaneous and starvation-induced
112 persistence. We found that endogenous ROS were generated following antibiotic exposure, and
113 that hypoxia significantly impaired bacterial killing. Thus, the lethality of some antibiotics is
114 amplified by toxic ROS accumulation, and persister cells require detoxification systems.
115
116 **RESULTS**
117 **Starvation-induced persister cell formation in mycobacteria**
118 We first sought to develop conditions suitable for genetic analysis of antibiotic persistence in
119 mycobacteria. Genetic screens examining persister cell physiology faces two inherent obstacles.
120 First, persister cells are rare in unstressed bacterial populations, and antibiotic-mediated cell
121 death creates population bottlenecks that obscure mutant phenotypes. Second, most
122 mycobacterial populations contain spontaneous drug-resistant mutants that can expand if the
123 population is exposed to a single antibiotic. To overcome these obstacles, we sought to establish
124 large-scale, high-density culture conditions to prevent genetic bottlenecks, and used multiple
125 antibiotics to suppress expansion of spontaneous drug-resistant mutants. We began by assessing
126 the feasibility of this approach using wild-type *Msmeg*. We exposed the cells to either the
127 combination of rifampin, isoniazid, and ethambutol (RIF/INH/EMB) used to treat *Mtb*, or to the
128 combination of tigecycline and linezolid (TIG/LZD), two translation-inhibiting antibiotics frequently
129 used to treat *Mabs*[27,35], and empirically determined the minimum-inhibitory concentrations (MICs)

each antibiotic under the high-density culture conditions that would be needed for genetic analysis of antibiotic persister cells. Both antibiotic combinations reduced the bacterial population >1000-fold within 72h (Figure 1A). We then evaluated both spontaneous and stress-induced persister cell formation under these conditions in *Msmeg*. We compared logarithmically growing (mid-log) cultures in 7H9 rich media to cultures starved for 2 days in PBS prior to addition of antibiotics. Consistent with expectations, we found a marked increase in the frequency of persister cells in starved cultures, with a 100-fold increase in survival following TIG/LZD exposure and a 10,000-fold increase following RIF/INH/EMB exposure (Figure 1A).

We next examined two species of pathogenic mycobacteria to similarly assess stress-induced persister formation under these conditions, as has been reported previously[36-39]. We again compared cells starved in PBS to mid-log cells growing 7H9, and found that cultures of wild-type *Mabs* (ATCC 19977 strain) and *Mtb* (Erdman) also displayed dramatic increases in the frequency of persister cells in nutrient-deprived cultures (Figure 1B,C). Notably, for *Mabs* and *Msmeg,* the development of these persister cells required an adaptation period of several days under starvation conditions, as formation of persister cells was dramatically impaired if cells were shifted immediately into nutrient-deficient conditions with antibiotics, suggesting that a regulated process needed to be completed (Figure 1D-F).

Identification of pathways needed for persister formation in *Mabs*

We used these conditions to carry out Tn-Seq screens in *Mabs* to identify genes necessary for forming both spontaneous and starvation-induced persister cells. We conducted the screen using a *Mabs Himar1* Tn library comprised of ~55,000 mutations across all 4,992 non-essential *Mabs* genes in strain ATCC 19977[29]. We maintained cells in log-phase growth in 7H9 rich media, or starved cells in PBS as described above, and then exposed them to TIG/LZD for 6 days (Figure 2A), a point at which spontaneous persister cells comprise the majority of the population (Figure

1C). Following antibiotic exposure cells were then washed and placed in antibiotic-free liquid media to recover, genomic DNA was isolated, and Tn insertion sites sequenced. We then used TRANSIT software[40] to quantify the abundance of each Tn mutant across different conditions and identify mutants with statistically-significant differences in distribution, in order to identify essential genes in both spontaneous and stress-induced antibiotic persister cells. We identified 277 *Mabs* genes required for surviving TIG/LZD exposure in rich media, 271 genes required for survival during starvation and 362 genes required to survive the combined exposure to antibiotics and starvation using criteria for significance of Log_2 fold-change > 0.5 and Benjamini–Hochberg adjusted p-value (p-adj.) ≤ 0.05 (Figure 2B-E). Of the genes required for antibiotic persistence, ~60% were required in both nutrient-replete and starvation states, although condition-specific determinants were also seen (Figure 2F). As expected, we identified genes with already-established functions in antibiotic responses, including MAB_2752 and MAB_2753 which are both homologs of known antibiotic transporters in *Mtb,* and tetracycline-responsive transcription factors such as MAB_4687 and MAB_0314c (Table S1), indicating an ability of these Tn-Seq conditions to identify physiologically relevant antibiotic-response genes.

To identify other cellular processes necessary for persister survival we performed pathway enrichment analysis on the set of genes identified by Tn-Seq. We used the DAVID[41] analysis tool to perform systematic queries of the KEGG, GO, and Uniprot databases and identify over-represented processes and pathways. Interestingly, although cells were exposed to translation-inhibiting antibiotics, and no exogenous oxidative or nitrosative stress was applied to the cells, we identified a number of factors needed to combat these stresses. This includes *bfrB* (bactoferritin), *ahpe* (peroxiredoxin) and *katG* (catalase/peroxidase) as well as 5 components of the bacterial proteasome pathway, known to mediate resistance to nitrosative stress in *Mtb*[42]. We also identified multiple members of DNA-damage response pathways including *recF*, *recG*, *uvrA*, *uvrB* and *uvrC* (Figure 2G, Table S2). Examining starvation-induced persisters, a number of the same

182 pathways were again seen, and the mutant with the greatest persister defect in this context was
183 *mntH*, a redox-regulated Mn/Zn transporter implicated in peroxide resistance in other organisms[43-
184 44]. Taken together, these findings suggest an unexpected scenario whereby translation inhibition
185 triggers accumulation of reactive oxygen or nitrogen species, with damage to macromolecules
186 such as DNA occurring.
187
188 We next sought to independently confirm a role in persister survival for genes identified by Tn-
189 Seq. We selected a set of genes with strong defects in persister formation, representing several
190 of the functional pathways identified, and used oligonucleotide-mediated recombineering
191 (ORBIT)[45] to disrupt their open reading frames. The initial genes selected were *pafA* (proteasome
192 pathway), *katG* (catalase-peroxidase), *recR* (DNA repair), *blaR* (β-lactam sensing), and
193 *MAB_1456c* (cobalamin synthesis). To control for non-specific effects of antibiotic selection during
194 the recombineering process, we created a control strain using ORBIT to target a non-coding
195 intergenic region downstream of a redundant tRNA gene (*MAB_t5030c*). We then individually
196 screened each of these mutants to determine if they displayed deficits in persister cell formation
197 by exposing cells to TIG/LZD, either in rich 7H9 media or under starvation conditions, as had been
198 done in the pooled Tn-Seq screen. For Δ*katG* we detected clear defects in persister cell survival
199 following 6 days of antibiotic exposure in either rich media or under starvation-induced conditions,
200 corroborating the results of our Tn-Seq analysis (Figure 3A). We observed smaller defects in the
201 Δ*pafA* and Δ*MAB_1456c* mutants (Figure 3B,C), and in *blaR* found no loss of overall viability, but
202 instead observed a delayed resumption of growth after removal of antibiotics (Figure 3D, data not
203 shown).
204 To further confirm the role of *katG* and *pafA,* and exclude off-target effects of recombineering, we
205 performed genetic complementation analysis by restoring a wild-type copy of each gene into the
206 respective Δ*pafA* and Δ*katG* mutants. In each case, we integrated a single copy of the wild-type

gene, under the control of its endogenous promoter, into the genome at the L5 *attB* site (hereafter *pafA+, katG+* strains), and constructed isogenic control strains with empty vector integrated at the same site (hereafter *pafA-, katG-* strains). We confirmed expression of the re-introduced copy of each gene by RT-qPCR in the *pafA+*, and *katG+* strains, and found expression within roughly 2-fold of endogenous wild-type levels (Figure 4A,D). We then challenged these strains with TIG/LZD as before. In rich media, where the Δ*katG* mutants have a moderate persistence defect, the *katG+* strain had roughly a 50-fold increase in viable cells relative to the *katG-* strain. We then exposed cells to antibiotics under starvation conditions, where the Δ*katG* mutant phenotype is more severe. Under these conditions the *katG-* cells succumbed rapidly between 3d and 10d after antibiotic exposure, with a 1,000-fold decrease in viable cells relative to control cells, whereas the *katG+* strain showed a near-complete restoration of persistence (Figure 4B). We analogously examined complementation of Δ*pafA* mutants, and although the phenotype of the Δ*pafA* mutant is less severe overall than a Δ*katG* mutant, we saw a similar restoration of survival in *pafA+* cells relative to *pafA-* cells (Figure 4E). We next evaluated whether the *pafA-*, and *katG-* strains were overall more sensitive to the growth inhibitory effects of TIG/LZD, or whether they had specific defects in survival above the mean bactericidal concentration. We performed MIC determination for TIG and LZD individually for each strain, comparing the *katG+*/*katG-* and *pafA+/pafA-* strains. We found that that the MICs for each of these strains were unchanged, demonstrating that these mutants were not more readily inhibited by these antibiotics. Instead, they have more rapid kinetics of cell death at bactericidal concentrations, consistent with a specific defect in antibiotic persistence (Figure 4C,F).

Reactive oxygen contributes to antibiotic lethality in *Mabs*

We next investigated the role of KatG in persister cell cells more broadly. We began by assessing whether *katG* conferred protection from other antibiotics with diverse mechanisms of action,

selecting antibiotics that are used clinically for mycobacterial infections. Because *katG*- mutants showed the greatest defects in starvation-induced persistence, we analyzed survival of *katG*+ and *katG*- strains in starvation-adapted cultures exposed to a panel of different antibiotics. Because both TIG and LZD both act by inhibiting translation, we began by exposing cells to either TIG or LZD alone. As expected, the degree of bacterial killing was significantly less with either agent alone than when they are added in combination. Upon exposure to either of these antibiotics the *katG*- cells died more rapidly than *katG*+ cells, though we note that the final proportion of persisters in the population was unchanged in *katG*- cells (Figure 5A). When we exposed cells to rifabutin (RFB), an RNA polymerase inhibitor, we saw a similar effect, with a 100-fold loss of viability in *katG*- cells relative to the *katG*+ cells (Figure 5B). In contrast, when we exposed cultures to either levofloxacin (gyrase inhibitor) or cefoxitin (β-lactam inhibitor of peptidoglycan cross-linking), *katG* had little to no effect on cell viability (Figure 5C-D). Thus, the role of KatG is context-dependent, suggesting that some antibiotics generate oxidative stress that can be ameliorated by KatG catalase/peroxidase activity while others do not.

The identification of *katG* as essential for persister cells to survive exposure to TIG/LZD suggests that ROS are present and causing damage. Although TIG/LIN are translation inhibitors that do not directly generate ROS we evaluated whether they might nonetheless be triggering ROS accumulation as a secondary effect. We examined ROS levels in *katG*+ *Mabs* using the ROS indicator dye cellROX, that is retained in cells when it becomes oxidized[46]. At baseline, during log-phase growth in rich media < 3% of cells had ROS accumulation (Figure 5E). We saw a moderate increase in ROS accumulation in starved cultures, with roughly 10% of the population cellROX+. However, when starved cultures were exposed to the TIG/LZD we saw a dramatic increase in ROS accumulation with over 30% cellROX+ cells. Taken together, these data indicate that translation inhibition does indeed have unanticipated downstream effects on cellular redox balance, with ROS accumulation that could be contributing to cell death.

We next tested whether ROS were contributing to cell death by reducing ROS production and assessing the impact on cell viability. A well-established system for studying hypoxia in mycobacteria is the Wayne Model of gradual-onset hypoxia, whereby low-density cultures are inoculated in sealed vessels with minimal headspace. As the culture slowly grows, the soluble O_2 is consumed, resulting in the onset of hypoxia over several days, a process that can be monitored by the decolorization of Methylene Blue dye in the media[47]. Under aerobic conditions in rich media, we observed the expected rapid killing of *Mabs* over the first 5 days with the combination of TIG/LZD, with more rapid loss of viability in KatG- cells. However, under hypoxic conditions, where ROS production is suppressed, we saw much slower bacterial killing. Importantly, under hypoxic conditions *katG*- cells no longer had a survival defect relative to *katG*+ cells, supporting the hypothesis that translation-inhibiting antibiotics also cause secondary accumulation of lethal ROS in antibiotic-treated cells that need to be detoxified by KatG (Figure 5F).

Incomplete penetrance of *katG* phenotype among *Mabs* strains

Finally, we tested the role of KatG in *Mabs* clinical strains to determine how widely the role of *katG* is conserved among different *Mabs* strains. We obtained 2 clinical isolates of *Mabs*, used ORBIT to disrupt the *katG* locus, and evaluated the ability of these strains to form both spontaneous and starvation-induced persister cells upon exposure to TIG/LZD. For clinical strain-1, the Δ*katG* mutant showed no defects in either condition (Figure 6B). In contrast, for clinical strain-2, *katG* contributed to starvation-induced persistence, as the Δ*katG* mutant rapidly lost viability in a manner similar to the ATCC 19977 reference strain. However, unlike ATCC 19977, this phenotype only manifested in starvation-induced persister cells, and was not seen in the absence of stress (Figure 6C). Thus, the *katG* phenotype displays incomplete penetrance, and the degree of protection it confers falls along a continuum among *Mabs* strains.

In summary, the results of these studies point to an important effect of ROS in amplifying the lethality of some antibiotics in *Mabs*. Through genetic analysis we identified a number of ROS detoxification factors, including KatG, as necessary for persisters to remain viable. This suggested that antibiotics might induce an oxidative state in cells, and direct measurement of ROS following antibiotic exposure indicated that this was indeed the case. Further supporting the deleterious effects of ROS in this context, we found that removal of oxygen both slowed bacterial killing and rendered KatG dispensable. Taken together these results suggest that antibiotic lethality is accelerated by toxic ROS accumulation, and persister survival requires active detoxification systems.

DISCUSSION:

Pathways necessary for persister formation in *Mabs.*

The phenomenon of bacterial persistence has been recognized for decades, and has been observed in a broad array of bacterial species. Despite this, a unifying mechanism of persister cell formation has not emerged, suggesting that different pathways may play a role in different contexts. A large body of work comes from *E. coli* where toxin-antitoxin systems such as HipBA[15], Lon protease[16,48] and the (p)ppGpp synthase RelA all contribute to the formation of persister cells[49-52]. However, even within this species other mechanisms seem to function, as RelA contributes to persister cell formation following exposure to β-lactams, but not quinolones[53]. In addition, how exactly these pathways maintain cell viability remains unclear. For example, while (p)ppGpp produced by RelA seems to act through Lon protease[16], the critical substrates in this process are note unknown. It is also unclear how mechanisms identified in one bacterial species may relate to the mechanisms in another. *RelA* plays a role in multiple species of bacteria, including *Pseudomonas aeruginosa*[54], *Staphylococcus aureus*[55], and *Mtb*[56]. However, the role of this pathway does not seem to be universal, as deletion of neither *relA* nor *lon* had an effect on persister formation in *Msmeg*[57]. Interestingly, in our Tn-Seq analysis, we did not identify *relA*.

309 However, a prior study of the *Mabs relA* mutant demonstrates that this strain still synthesizes
310 (p)ppGpp[58], suggesting genetic redundancy and a need to disrupt additional genes in a *relA*
311 mutant in order to study the role of (p)ppGpp in *Mabs*.
312
313 **Mechanisms of antibiotic lethality**
314 The mechanisms of bacterial cell death following antibiotic exposure remains somewhat
315 controversial. The most straightforward explanation is that antibiotics kill by directly disrupting the
316 function of their targets. However, more recently it was suggested that antibiotics kill through a
317 final common pathway of lethal ROS generation, leading to oxidative damage of DNA and other
318 macromolecules[59]. Since that time, there have been studies, both supporting[10,19-20] and refuting
319 the role of ROS[21-22] in antibiotic-mediated cell death.
320
321 Our analysis of *Mabs* persister cells provides new insights. The identification of multiple genes
322 involved in ROS detoxification through an unbiased genome-wide screen suggests that ROS also
323 promotes antibiotic lethality in *Mabs*. This idea is further supported by the detection of elevated levels
324 of ROS after exposure to translation inhibitors, and that removal of oxygen slowed antibiotic killing.
325 Taken together, these data strongly support the idea that ROS are a significant contributor to
326 antibiotic lethality in some contexts. These findings are supported by other published studies in
327 mycobacteria. In *Mabs* and *Msmeg,* other groups have also observed reduced antibiotic-mediated
328 killing in hypoxic conditions[10,36]. In *Mtb*, exposure to rifampin also generates ROS[19,60], and *katG*
329 contributes to survival in rifampin-treated cells[19].
330
331 The source of ROS under these conditions is uncertain. In principle, any of several derangements
332 could lead to ROS accumulation. One of the major sources of cellular ROS is oxidative
333 phosphorylation, as hydrogen peroxide, superoxide, and hydroxyl radicals are natural byproducts.
334 Thus, increased ROS generation by oxidative phosphorylation is an attractive hypothesis.

Alternatively, particularly under starvation conditions, it is possible that antioxidants and ROS scavengers may become depleted, creating a more oxidizing environment. Our Tn-Seq analysis provides additional insight on this. We noted a small class of Tn mutants that were paradoxically protected from antibiotic lethality (Figure 2B). Prominent among this class of mutants were several independent components of the NADH dehydrogenase complex (Table S1). Also known as Complex I of the electron transport chain, it is one of the key entry points for electrons into the oxidative phosphorylation pathway. The observation that mutants in this complex are protected suggests that decreasing flux through oxidative phosphorylation, with a concomitant decrease in ROS generation, may enhance survival during antibiotic exposure.

However, antibiotic-induced ROS accumulation is not a universal phenomenon. With some antibiotics we examined in *Mabs,* loss of *katG* had no effect. In addition, ROS detoxification does not always play a protective role, as loss of catalase and peroxidase activities in *E. coli* also had no effect on persister survival[22]. Taken together, this suggests a model in which antibiotics cause direct toxicity by acting on their target, but in addition, some antibiotics, notably transcription inhibitors and translation inhibitors, also appear to have a secondary toxic effect of causing ROS accumulation. How exactly transcription or translation blockade leads to increased ROS levels is currently unclear and will require further investigation, although our data suggest that the electron transport chain might play an important role.

Therapeutic implications

Mabs infections are particularly challenging to eradicate, with relapse rates over 50%[28]. Our results highlight several bacterial processes such as the bacterial proteasome or ROS detoxification that might be targeted therapeutically to reduce the development or survival of persister cells. Agents targeting these process might not have any intrinsic antimicrobial activity alone, but might act to target the unique physiology of persister cells that develop upon antibiotic

exposure. This would represent a new therapeutic class of “persistence inhibitors” that might act synergistically with traditional antibiotics to eliminate the subpopulation of persister cells that would otherwise remain viable despite prolonged antibiotic exposure in *Mabs* and other chronic infections.

Limitations

Tn-Seq has inherent drawbacks, including an inability to identify mutants in essential genes, or in cases of genetic redundancy. Thus, there are likely genes needed for antibiotic persistence in *Mabs* that were not identified in this study. In addition, we studied the response to a single class of antibiotic, focusing on the translation inhibitors often used to treat *Mabs* infections, and we studied only spontaneous and starvation-induced persister cells. It is likely that studying other antibiotics, with different mechanisms of action, or different stresses that induce persister cells, would identify additional genes contributing to persister formation and would allow better identification of core survival pathways that might be shared among different forms of stress.

MATERIALS AND METHODS

Key Reagent Table

Reagent	Source/Reference	Identifier
***Mabs* ATCC 19977**	ATCC	19977
***Msmeg* MC2 155**	ATCC	700084
***Mtb* Erdman**	ATCC	35801
***Mabs* clinical strains**	Sacramento Department of Public Health	NA
pkm444	Addgene	108319
pkm496	Addgene	109301

pmv306	Ref. 61	
Middlebrook 7H9	BD	271310
Middlebrook 7H10	BD	262710
Glycerol	Invitrogen	15514011
Tween-80	Fisher	BP338-500
Middlebrook OADC	BD	212351
DPBS (-Ca/Mg)	Gibco	14190144
Tyloxapol	Sigma Aldrich	T8761
Methylene blue	Sigma Aldrich	28514
Tigecycline	Chem Impex	29737
Linezolid	Chem Impex	29723
Levofloxacin	Sigma Aldrich	28266
Cefoxitin	Chem Impex	1490
Rifabutin	Cayman Chemical	16468
Rifampin	Sigma Aldrich	R7382
Isoniazid	Supelco	I3377
Ethambutol	Thermo Scientific	J6069506
DMSO	Sigma Aldrich	D2650
Trizol	Invitrogen	15596018
0.1mm zirconia beads	Biospec	11079101z
PureLink RNA Mini Kit	Invitrogen	12183025
Kanamycin	VWR	75856-686
Zeocin	Invivogen	ANTZN1P
Glycine	Fisher Bioreagents	BP381
Sucrose	Sigma Aldrich	S1888

Anhydrotetracycline	Cayman Chemical	10009542
cellROX green	Invitrogen	C10444
Paraformaldehyde	Sigma Aldrich	P6148
DAPI	Sigma Aldrich	D9542
DNAseI	New England Biolabs	M0303
Maxima H minus reverse transcriptase	Thermo Scientific	EP0752
Taq Polymerase	New England Biolabs	M0273
EvaGreen	Biotium	31019

Bacterial strains and culture conditions:

Mabs ATCC 19977, clinical *Mabs* strains and *Msmeg* (MC2 155) were grown in BD Middlebrook 7H9 media (liquid) or 7H10 media (solid) supplemented with 0.5% glycerol (Sigma) and 0.2% Tween-80 (Fisher) but without any OADC supplementation except for transformations. Sacramento clinical isolates were obtained from the Sacramento County Department of Public Health Mycobacteriology Laboratory. Confirmation of clinical isolates as *Mabs* was performed by amplifying the 16s rRNA locus and Sanger sequencing. *Mtb* (Erdman) was grown in 7H9 (liquid) or 7H10 (solid) supplemented with 0.5% glycerol, 0.1% Tween-80, and 10% OADC (BD). All cultures were grown at 37°C with gentle shaking. Except for specific hypoxia conditions, all liquid cultures were grown with 90% container headspace or using a gas permeable cap to ensure culture oxygenation. PBS starvation was achieved by washing OD0.5-1.0 *Mabs* 1X in DPBS (-Ca/Mg, Gibco) and resuspending in DPBS at OD=1, supplemented with 0.1% tyloxapol (Sigma).

Mabs antibiotic experiments:

For PBS starvation experiments, stocks of *Mabs* were grown for 48 hours in 7H9 passaging continuously in log phase, then PBS starved or passaged in log phase for an additional 48h. Log phase or PBS starved *Mabs* were then resuspended in antibiotic containing media at OD1.0. For experiments with hypoxia, *Mabs* in mid-log aerobic growth was adjusted to OD0.001 in media with 1.5ug/ml methylene blue and added to a rubber septum sealed glass vial with 50% headspace. Methylene blue discoloration was observed at 3d and antibiotics were added at 5d. We empirically determined the half-life of each antibiotic in 7H9 media at 37-deg and for those with half-lives shorter than the experiment, supplemented cultures to with additional antibiotic to maintain the concentration of active antibiotic. Antibiotics were used at the following concentrations: tigecycline (Chem-Impex) at 10ug/ml (8 fold above MIC, re-administered every 3 days), linezolid (Chem-Impex) at 100ug/ml (20 fold above MIC), levofloxacin (Sigma) at 40ug/ml (8 fold above MIC), cefoxitin (Chem Impex) at 80ug/ml (8 fold above MIC, re-administered every 3 days), and rifabutin (Cayman) at 40ug/ml (4 fold above MIC). After antibiotic administration, colony forming units over time were measured.

Msmeg antibiotic experiments:

Individual colonies were picked and grown for 48 hours in log phase before being PBS starved or passaged in log phase for 48h. Log phase or PBS starved *Msmeg* were then resuspended in antibiotic containing media at OD1.0. Antibiotics were used at the following concentrations: tigecycline (Chem-Impex) at 1.25ug/ml (8 fold above MIC, re-administered every 3 days), linezolid (Chem-Impex) at 2.5ug/ml (8 fold above MIC), rifampin (Sigma) at 32ug/ml (8 fold above MIC, re-administered every 6 days), isoniazid (Sigma) at 32ug/ml (8 fold above MIC, re-administered every 6 days), and ethambutol (Thermo) at 4ug/ml (8 fold above MIC, re-administered every 3 days). After antibiotic administration, colony forming units over time were measured.

Mtb antibiotic experiments:

Freezer stocks of *Mtb* were thawed and grown for 5-7 days in log phase before being starved for 14d or longer. Non-starved control *Mtb* were thawed such that they were also grown for 5-7 days in log phase before experimental use. Log phase or PBS starved *Mtb* was then resuspended in antibiotic containing media and adjusted to OD1.0. Antibiotics were used at the following concentrations: rifampin (Sigma) at 0.1ug/ml (4 fold above MIC, re-administered every 6 days), isoniazid (Sigma) at 0.1ug/ml (4 fold above MIC, re-administered every 6 days), and ethambutol (Thermo) at 8ug/ml (4 fold above MIC, re-administered every 6 days). After antibiotic administration, colony forming units over time were measured.

Transposon insertion sequencing:

The construction of this *Himar1* transposon Tn library has been described previously [29]. Screening was performed by growing a freezer stock of the library for 2.5 days in log phase before 48-hour PBS starvation or further continuous log-phase growth. Samples were then resuspended in media containing either tigecycline/linezolid or an equal volume of DMSO solvent and incubated for 6 days, with a re-administration of tigecycline or matching DMSO on day 3. The samples were then washed 2X in antibiotic free liquid media, resuspended in antibiotic free liquid media (10X the original culture volume), and grown until OD0.5-1.0. Subsequently, the samples underwent three more rounds of 100-fold passaging in liquid media to amplify surviving bacteria before the samples were collected in Trizol (Invitrogen). A sample taken at the time of the commencement of PBS starvation was collected in Trizol and used as the input control. Three independent trials of this experiment were submitted to the UC Davis DNA Technologies Core, where Tn insertion site flanking sequences were amplified as described previously [29] and sequenced on sequenced on an Illumina AVITI. Sequence reads were mapped to the ATCC 19977 genome and analyzed using TRANSIT software with the following parameters: 0% of N/C termini ignored, 10,000 samples, TTR normalization, LOESS correction, include sites with all zeros, site restricted

resampling. Genes with significant changes were defined as those with adjusted p-value (p-adj.) <0.05 and $\log_2$ fold change >0.5. P-adj. was calculated using the Benjamini-Hochberg correction.

Pathway enrichment analysis

To improve gene annotation, *Mabs* orthologs to *Mtb* genes were identified. *Mabs* genes were first converted into protein sequences using Mycobrowser, and protein sequences were then used to perform reciprocal BLASTp searches. *Mabs* genes and *Mtb* genes that mapped to each other using independent one-way BLASTp searches with a maximum e-value cutoff of 0.1 were considered orthologs. For pathway analysis, gene lists (*Mtb* orthologs) were then imported into the DAVID knowledgebase[41] and pathway enrichment analysis performed for Gene Ontology biological process, Uniprot keyword and KEGG databases with statistical analysis Fisher's exact test and nominal p-value reported.

Gene deletion and complementation:

Knockout strains were generated using ORBIT[45]. Briefly, *Mabs* was transformed with the kanamycin-resistant ORBIT recombineering plasmid pkm444. 20ml *Mabs* at OD0.5-1.0 was washed 2X in 10% glycerol and resuspended in 200ul 10% glycerol. 500ng plasmid was added and electroporated at 2.5kV in 0.2cm cuvettes. The bacteria were allowed to recover overnight before plating on 150ug/ml kanamycin plates. Clones were selected and regrown in liquid media supplemented with 150ug/ml kanamycin and 10% OADC (BD) to OD0.5-1.0. For recombineering, the pkm444-*Mabs* was grown to mid-log, then diluted to OD0.1 and 200mM glycine (Fisher) was added to the media. 16 hours later, 500mM sucrose (Sigma) and 500ng/ml anhydrotetracycline (Cayman) were added and incubated for an additional 4 hours. Subsequently, the *Mabs* was washed 2X in ice cold 10% glycerol + 500mM sucrose. 200ul of 10X concentrated *Mabs* was then electroporated with 600ng of the zeocin-R ORBIT payload pkm496 plasmid and 2ug of targeting oligonucleotide (Table S3) at 2.5kV in 0.2cm cuvettes. The *Mabs* was then allowed to recover

overnight in liquid media with 10% OADC and 500ng/ml anhydrotetracycline before being plated on 150ug/ml zeocin plates. Mutants were then selected and screened for gene deletion by PCR amplification and Sanger sequencing. For genetic complementation, the endogenous loci including promoter and terminator sequences were amplified by PCR and cloned into the EcoRV site of pmv306 with kanamycin resistance[61]. In the case of *katG,* the upstream gene *furA* was also included in the complementation construct to achieve optimal *katG* expression.

MIC analysis

Two-fold serial dilutions of antibiotics were prepared in a 96 well plate in 100ul volume. 100ul of 2X bacteria were added (for *Mabs*: used a final OD of 0.001, *Msmeg*: OD0.001, *Mtb*: OD0.01), making a final volume of 200ul. The plates were incubated until there was visible growth in the no antibiotic control well. At this time, the bacteria were transferred to a new plate with 20ul of 40% paraformaldehyde and OD620 measurements were taken with a FilterMax F3 plate reader (Molecular Devices).

Flow cytometry

OD1 Mab was stained with cellROX green (Invitrogen) at a final concentration of 5uM for 1hr at 37C. The cells were then washed in PBS and resuspended in PBS with 4% paraformaldehyde and 5ug/ml DAPI (Sigma). The samples were run on a LSRII flow cytometer (BD). Fluorophores were excited with the 405nm (DAPI) and 488nm (cellROX) lasers. Detection was performed using the 450/50 (505LP) filter for DAPI and a 525/50 (555LP) filter for cellROX. Data were analyzed with FlowJo software (BD).

DNA/RNA Purification:

Samples were resuspended in 5 volumes of Trizol and were bead beat with 0.1mm zirconia beads (Biospec) 6x2min at 4°C in a Mini-Beadbeater-16 (Biospec). Chloroform was added and RNA in the aqueous phase removed. For DNA isolation, a second RNA extraction was performed with 0.8M guanidine thiocyanate and 0.5M guanidine hydrochloride, 60mM Acetate pH 5.2, 1mM EDTA. DNA was then isolated with back-extraction buffer (4M Guanidine Thiocyanate, 50mM Sodium Citrate, 1M Tris base (without pH adjustment ~pH 11) and DNA purified using a PureLink RNA Mini Kit (Invitrogen).

RT-qPCR

RNA was purified using PureLink RNA Mini Kit per manufacturer's instructions. The samples were DNAseI (NEB) treated for 15min/37°C before stopping the reaction by adding 3.5mM EDTA and heating for 10min/75°C. cDNA was synthesized from 500ng total RNA using random hexamers and Maxima H minus reverse transcriptase (Thermo). No reverse-transcription controls were also included and used to confirm the lack of genomic DNA-driven amplification. qPCR reactions used Taq polymerase (NEB) and EvaGreen (Biotium) and were run on Biorad CFX Opus 96 Real-Time PCR System. Melt curves were included for each sample to confirm uniform amplicon identity between samples. Gene-specific amplification was quantified by comparison to a standard curve generated from 3-fold serial dilutions of a control sample, then normalized to 16S rRNA within each sample.

FIGURE LEGENDS

Figure 1. Starvation induces antibiotic persister cells across diverse mycobacteria. (A) *Msmeg,* (B) *Mtb* or (C) *Mabs* were grown in 7H9 rich media or starved in PBS prior to the addition of the indicated antibiotics. Cells were allowed to adapt to starvation for a period of 48h for *Msmeg* and *Mabs* and 14-21d for *Mtb* prior to the addition of antibiotics in PBS where indicated. (D-F) As above, but with/without a period of adaptation in PBS prior to antibiotics as indicated. Antibiotic

concentrations were: *Msmeg* - Isoniazid (INH) 32ug/ml (8 x MIC), rifampin (RIF) 32ug/ml (8 x MIC), ethambutol (EMB) 4ug/ml (8 x MIC), tigecycline (TIG) 1.25ug/ml (8 x MIC), linezolid (LZD) 2.5ug/ml (8 x MIC). *Mtb* – RIF 0.1ug/ml (4 x MIC), INH at 0.1ug/ml (4 x MIC), EMB at 8ug/ml (4 x MIC). *Mabs* – TIG (8 x MIC), LZD 100ug/ml (20 x MIC). Antibiotics with half-lives shorter than the duration of experiment were re-added at the following intervals: TIG, EMB every 3d; RIF, INH every 6d. Error bars represent SEM, statistical significance is calculated at each time point using student's t test. ****: $p<0.0001$, ***: $p<0.001$, **: $p<0.01$, *: $p<0.05$, ns: $p>0.05$. Data are combined from 3 independent experiments.

Figure 2. Tn-Seq identifies genes required for antibiotic persistence in *Mabs*. (A) Experimental design. (B-E) Tn-Seq analysis showing relative abundance of individual genes under the indicted conditions. All cultures were fully aerated throughout the experiment and cultures without antibiotics received and equal volume of DMSO. For (B-D) gene abundance in the indicated condition is measured relative the input log-phase population. In (E) an additional comparison is made relative to the PBS condition. Genes with significant decreases in abundance are shown in color (p-adj. < 0.05 and $\log_2$ fold-change > 0.5) using the Benjamini–Hochberg adjustment for multiple hypothesis testing. (F) Number of genes essential in each condition relative to the input population. (G) Pathway enrichment analysis of the essential genes in each condition using the DAVID knowledgebase ($p<0.05$). Screens were run as 3 independent experiments and the combined results analyzed. Antibiotic conditions were used as described in Figure 1.

Figure 3. Independent deletions of *katG* and *pafA* confirm Tn-Seq results. (A-E) ORBIT recombineering was used to disrupt the indicated genes, or to generate a control strain with an intergenic region targeted distal to tRNA gene *MAB_t5030c*. Each mutant was either grown in 7H9 rich media or starved in PBS for 48 prior to the addition of antibiotics. Error bars represent

SEM, statistical significance is calculated at each time point using student's t test. ****: p<0.0001, ***: p<0.001, **: p<0.01, *: p<0.05, ns: p>0.05. Antibiotics were added as described above. Data are combined from 4 independent experiments.

Figure 4. Complementation analysis *katG* and *pafA* mutants confirms their role in persister survival. (A) RT-qPCR analysis of *katG* expression in *katG- (ΔkatG::pmv306), katG+ (ΔkatG::pmv306 katG),* and control strain (ORBIT intergenic*::pmv306).* (B) CFU over time for *katG+/katG-* strains. (C) MICs for *katG+/katG-* strains. (D) Expression of *pafA in pafA- (ΔpafA::pmv306), pafA+ (pafA::pmv306 pafA)* and control strains. (E) CFU over time of *pafA+/pafA-* strains. (F) MICs for *pafA+/pafA-* strains. Antibiotic concentrations in (A-B, D-E) are as described above. Error bars represent SEM, statistical significance is calculated at each time point using student's t test between *katG+/katG-* strains in (B) and between *pafA+/pafA-* strains in (E). ****: p<0.0001, ***: p<0.001, **: p<0.01, *: p<0.05, ns: p>0.05. Antibiotics were added as described above.

Figure 5. ROS-mediated toxicity following antibiotic exposure. (A-D) Analysis of *katG+/katG-* cells challenged with different antibiotics. Cells were starved in PBS for 48h and then exposed to the indicated antibiotic. (E) Flow cytometry of cells *katG*$^{+}$ cells stained with DAPI and the ROS-sensitive dye cellROX after 72h in the indicated conditions. Percentage cellROX-positive cells are shown. (F) Persister survival over time for aerated and hypoxic and cultures of *Mabs* after exposure to TIG/LIN. Error bars represent SEM, statistical significance is calculated at each time point using student's t test. ****: p<0.0001, ***: p<0.001, **: p<0.01, *: p<0.05, ns: p>0.05. (A-D) are combined data from 3 independent experiments. (E) are representative (median) data from 3 independent experiments. (F) are combined data from 4 independent experiments. Antibiotics were added as described above.

Figure 6. Incomplete penetrance of *katG* phenotype among *Mabs* strains. Δ*katG* strains and control strains targeting an intergenic region were constructed on the indicated *Mabs* backgrounds using ORBIT recombineering: (A) ATCC 19977, (B-C) clinical strains. Bacteria were cultured in 7H9 or starved for 48h in PBS and then treated with antibiotics where indicated. Cultures without antibiotics received an equal volume of DMSO as a control. Survival over time is shown. Error bars represent SEM, statistical significance is calculated at each time point using student's t test. ****: p<0.0001, ***: p<0.001, **: p<0.01, *: p<0.05, ns: p>0.05.Combined data from 4 independent experiments are shown. Antibiotics were added as described above.

Table S1. Tn-Seq results

Table S2. DAVID functional pathway analysis

Table S3. Oligonucleotide sequences

ACKNOWLEDGEMENTS

We would like to thank Nick Campbell-Kruger for his technical insights on identifying *Mabs/Mtb* orthologs, Jonathan Van Dyke for his assistance with flow cytometry analysis, Emily Kumimoto and Siranoosh Ashtari for their assistance with Tn-Seq library preparation and sequencing, and Jessie Li and Bradley Jenner for their assistance with Tn-seq bioinformatics. We would also like to thank Caroline Dominic at the Sacramento County Department of Public Health for providing clinical isolates of *Mabs* for analysis.

FUNDING

Pew Biomedical Fellowship BHP

NIH RO1 1R01AI144149 BHP

NIH R01 1R01AI143722 SAS

NIH Shared Instrumentation Grant 1S10OD010786-01 DNA Technologies and Expression Analysis Core, UC Davis Genome Center

NCI Cancer Center Support Grant P30CA093373 Flow Cytometry Shared Resource, UC Davis

CONFLICTS OF INTEREST

BHP and SAS serve on the scientific advisory board of X-Biotics Therapeutics.

REFERENCES

1. Stevens, D.L., A.L. Bisno, H.F. Chambers, E.P. Dellinger, E.J. Goldstein, S.L. Gorbach, J.V. Hirschmann, S.L. Kaplan, J.G. Montoya, and J.C. Wade, *Practice guidelines for the diagnosis and management of skin and soft tissue infections: 2014 update by the Infectious Diseases Society of America.* Clin Infect Dis, 2014. **59**(2): p. e10-52.
2. Metersky, M.L. and A.C. Kalil, *Management of ventilator-associated pneumonia: guidelines.* Clinics in chest medicine, 2018. **39**(4): p. 797-808.
3. Meylan, S., I.W. Andrews, and J.J. Collins, *Targeting Antibiotic Tolerance, Pathogen by Pathogen.* Cell, 2018. **172**(6): p. 1228-1238.
4. Namugenyi, S.B., A.M. Aagesen, S.R. Elliott, and A.D. Tischler, *Mycobacterium tuberculosis PhoY Proteins Promote Persister Formation by Mediating Pst/SenX3-RegX3 Phosphate Sensing.* mBio, 2017. **8**(4): p. e00494-17.
5. Liu, Y., S. Tan, L. Huang, R.B. Abramovitch, K.H. Rohde, M.D. Zimmerman, C. Chen, V. Dartois, B.C. VanderVen, and D.G. Russell, *Immune activation of the host cell induces drug tolerance in Mycobacterium tuberculosis both in vitro and in vivo.* Journal of Experimental Medicine, 2016. **213**(5): p. 809-825.
6. Gold, B. and C. Nathan, *Targeting Phenotypically Tolerant Mycobacterium tuberculosis.* Microbiol Spectr, 2017. **5**(1).

7. Bigger, J.J.T.L., *Treatment of staphylococcal infections with penicillin by intermittent sterilisation.* 1944. **244**(6320): p. 497-500.

8. Ronneau, S., P.W.S. Hill, and S. Helaine, *Antibiotic persistence and tolerance: not just one and the same.* Current opinion in microbiology, 2021. **64**: p. 76-81.

9. Dhar, N. and J.D. McKinney, *Microbial phenotypic heterogeneity and antibiotic tolerance.* Current opinion in microbiology, 2007. **10**(1): p. 30-38.

10. Grant, S.S., B.B. Kaufmann, N.S. Chand, N. Haseley, and D.T. ng, *Eradication of bacterial persisters with antibiotic-generated hydroxyl radicals.* Proceedings of the National Academy of Sciences, 2012. **109**(30): p. 12147-12152.

11. Baker, J.J. and R.B. Abramovitch, *Genetic and metabolic regulation of Mycobacterium tuberculosis acid growth arrest.* Scientific Reports, 2018. **8**(1).

12. Saito, K., T. Warrier, S. Somersan-Karakaya, L. Kaminski, J. Mi, X. Jiang, S. Park, K. Shigyo, B. Gold, and J. Roberts, *Rifamycin action on RNA polymerase in antibiotic-tolerant Mycobacterium tuberculosis results in differentially detectable populations.* Proceedings of the National Academy of Sciences, 2017. **114**(24): p. E4832-E4840.

13. Hipolito, V.E.B., E. Ospina-Escobar, and R.J. Botelho, *Lysosome remodelling and adaptation during phagocyte activation.* Cell Microbiol, 2018. **20**(4).

14. Sukumar, N., S. Tan, B.B. Aldridge, and D.G. Russell, *Exploitation of Mycobacterium tuberculosis reporter strains to probe the impact of vaccination at sites of infection.* PLoS Pathog, 2014. **10**(9): p. e1004394.

15. Schumacher, M.A., K.M. Piro, W. Xu, S. Hansen, K. Lewis, and R.G. Brennan, *Molecular Mechanisms of HipA-Mediated Multidrug Tolerance and Its Neutralization by HipB.* Science, 2009. **323**(5912): p. 396-401.

16. Harms, A., C. Fino, A. Sørensen Michael, S. Semsey, and K. Gerdes, *Prophages and Growth Dynamics Confound Experimental Results with Antibiotic-Tolerant Persister Cells.* mBio, 2017. **8**(6): p. 10.1128/mbio.01964-17.

17. Korch, S.B., T.A. Henderson, and T.M. Hill, *Characterization of the hipA7 allele of Escherichia coli and evidence that high persistence is governed by (p)ppGpp synthesis.* Mol Microbiol, 2003. **50**(4): p. 1199-213.

18. Wong, F., S. Wilson, R. Helbig, S. Hegde, O. Aftenieva, H. Zheng, C. Liu, T. Pilizota, E.C. Garner, A. Amir, and L.D. Renner, *Understanding Beta-Lactam-Induced Lysis at the Single-Cell Level.* Frontiers in Microbiology, 2021. **12**.

19. Saito, K., S. Mishra, T. Warrier, N. Cicchetti, J. Mi, E. Weber, X. Jiang, J. Roberts, A. Gouzy, E. Kaplan, C.D. Brown, B. Gold, and C. Nathan, *Oxidative damage and delayed replication allow viable Mycobacterium tuberculosis to go undetected.* Sci Transl Med, 2021. **13**(621): p. eabg2612.

20. Vilchèze, C., T. Hartman, B. Weinrick, P. Jain, T.R. Weisbrod, L.W. Leung, J.S. Freundlich, and W.R. Jacobs, Jr., *Enhanced respiration prevents drug tolerance and drug resistance in Mycobacterium tuberculosis.* Proc Natl Acad Sci U S A, 2017. **114**(17): p. 4495-4500.

21. Keren, I., S. Minami, E. Rubin, and K. Lewis, *Characterization and transcriptome analysis of Mycobacterium tuberculosis persisters.* mBio, 2011. **2**(3): p. e00100-11.

22. Liu, Y. and J.A. Imlay, *Cell death from antibiotics without the involvement of reactive oxygen species.* Science, 2013. **339**(6124): p. 1210-3.

23. de Keijzer, J., A. Mulder, J. de Beer, A.H. de Ru, P.A. van Veelen, and D. van Soolingen, *Mechanisms of Phenotypic Rifampicin Tolerance in Mycobacterium tuberculosis Beijing Genotype Strain B0/W148 Revealed by Proteomics.* J Proteome Res, 2016. **15**(4): p. 1194-204.

24. Gold, B., T. Warrier, and C. Nathan, *A multi-stress model for high throughput screening against non-replicating Mycobacterium tuberculosis.* Mycobacteria protocols, 2015: p. 293-315.

674 25. Dorman, S.E., P. Nahid, E.V. Kurbatova, P.P. Phillips, K. Bryant, K.E. Dooley, M. Engle,
675 S.V. Goldberg, H.T. Phan, and J. Hakim, *Four-month rifapentine regimens with or without*
676 *moxifloxacin for tuberculosis.* New England Journal of Medicine, 2021. **384**(18): p. 1705-
677 1718.
678 26. Nahid, P., S.E. Dorman, N. Alipanah, P.M. Barry, J.L. Brozek, A. Cattamanchi, L.H.
679 Chaisson, R.E. Chaisson, C.L. Daley, and M. Grzemska, *Official American thoracic*
680 *society/centers for disease control and prevention/infectious diseases society of America*
681 *clinical practice guidelines: treatment of drug-susceptible tuberculosis.* Clinical infectious
682 diseases, 2016. **63**(7): p. e147-e195.
683 27. Griffith, D.E., T. Aksamit, B.A. Brown-Elliott, A. Catanzaro, C. Daley, F. Gordin, S.M.
684 Holland, R. Horsburgh, G. Huitt, and M.F. Iademarco, *An official ATS/IDSA statement:*
685 *diagnosis, treatment, and prevention of nontuberculous mycobacterial diseases.*
686 American journal of respiratory and critical care medicine, 2007. **175**(4): p. 367-416.
687 28. Griffith, D.E. and C.L. Daley, *Treatment of Mycobacterium abscessus Pulmonary*
688 *Disease.* CHEST, 2022. **161**(1): p. 64-75.
689 29. Rodriguez, R., N. Campbell-Kruger, J. Gonzalez Camba, J. Berude, R. Fetterman, and
690 S. Stanley, *MarR-Dependent Transcriptional Regulation of mmpSL5 Induces*
691 *Ethionamide Resistance in Mycobacterium abscessus.* Antimicrobial Agents and
692 Chemotherapy, 2023. **67**(4): p. e01350-22.
693 30. Li, S., N.C. Poulton, J.S. Chang, Z.A. Azadian, M.A. DeJesus, N. Ruecker, M.D.
694 Zimmerman, K.A. Eckartt, B. Bosch, C.A. Engelhart, D.F. Sullivan, M. Gengenbacher,
695 V.A. Dartois, D. Schnappinger, and J.M. Rock, *CRISPRi chemical genetics and*
696 *comparative genomics identify genes mediating drug potency in Mycobacterium*
697 *tuberculosis.* Nature microbiology, 2022. **7**(6): p. 766-779.
698 31. Carey, A.F., J.M. Rock, I.V. Krieger, M.R. Chase, M. Fernandez-Suarez, S. Gagneux,
699 J.C. Sacchettini, T.R. Ioerger, and S.M. Fortune, *TnSeq of Mycobacterium tuberculosis*

clinical isolates reveals strain-specific antibiotic liabilities. PLoS pathogens, 2018. **14**(3): p. e1006939.

32. Kreutzfeldt, K.M., R.S. Jansen, T.E. Hartman, A. Gouzy, R. Wang, I.V. Krieger, M.D. Zimmerman, M. Gengenbacher, J.P. Sarathy, M. Xie, V. Dartois, J.C. Sacchettini, K.Y. Rhee, D. Schnappinger, and S. Ehrt, *CinA mediates multidrug tolerance in Mycobacterium tuberculosis.* Nat Commun, 2022. **13**(1): p. 2203.

33. Block, A.M., S.B. Namugenyi, N.P. Palani, A.M. Brokaw, L. Zhang, K.B. Beckman, and A.D. Tischler, *Mycobacterium tuberculosis Requires the Outer Membrane Lipid Phthiocerol Dimycocerosate for Starvation-Induced Antibiotic Tolerance.* Msystems, 2023. **8**(1): p. e0069922.

34. Bellerose, M.M., S.-H. Baek, C.-C. Huang, C.E. Moss, E.-I. Koh, M.K. Proulx, C.M. Smith, R.E. Baker, J.S. Lee, S. Eum, S.J. Shin, S.-N. Cho, M. Murray, and C.M. Sassetti, *Common Variants in the Glycerol Kinase Gene Reduce Tuberculosis Drug Efficacy.* mBio, 2019. **10**(4): p. e00663-19.

35. Kumar, K., C.L. Daley, D.E. Griffith, and M.R. Loebinger, *Management of Mycobacterium avium complex and Mycobacterium abscessus pulmonary disease: therapeutic advances and emerging treatments.* European respiratory review, 2022. **31**(163).

36. Yam, Y.K., N. Alvarez, M.L. Go, and T. Dick, *Extreme Drug Tolerance of Mycobacterium abscessus "Persisters".* Front Microbiol, 2020. **11**: p. 359.

37. Berube, B.J., L. Castro, D. Russell, Y. Ovechkina, and T. Parish, *Novel Screen to Assess Bactericidal Activity of Compounds Against Non-replicating Mycobacterium abscessus.* Front Microbiol, 2018. **9**: p. 2417.

38. Lee, J., N. Ammerman, A. Agarwal, M. Naji, S.Y. Li, and E. Nuermberger, *Differential In Vitro Activities of Individual Drugs and Bedaquiline-Rifabutin Combinations against Actively Multiplying and Nutrient-Starved Mycobacterium abscessus.* Antimicrob Agents Chemother, 2021. **65**(2).

726 39. Betts, J.C., P.T. Lukey, L.C. Robb, R.A. McAdam, and K. Duncan, *Evaluation of a*
727 *nutrient starvation model of Mycobacterium tuberculosis persistence by gene and protein*
728 *expression profiling.* Molecular Microbiology, 2002. **43**(3): p. 717-731.
729 40. DeJesus, M.A., C. Ambadipudi, R. Baker, C. Sassetti, and T.R. Ioerger, *TRANSIT-a*
730 *software tool for Himar1 TnSeq analysis.* PLoS computational biology, 2015. **11**(10): p.
731 e1004401.
732 41. Huang da, W., B.T. Sherman, and R.A. Lempicki, *Systematic and integrative analysis of*
733 *large gene lists using DAVID bioinformatics resources.* Nat Protoc, 2009. **4**(1): p. 44-57.
734 42. Darwin, K.H., S. Ehrt, J.-C. Gutierrez-Ramos, N. Weich, and C.F. Nathan, *The*
735 *proteasome of Mycobacterium tuberculosis is required for resistance to nitric oxide.*
736 Science, 2003. **302**(5652): p. 1963-1966.
737 43. Shi, H., R. Zhang, L. Lan, Z. Chen, and J. Kan, *Zinc mediates resuscitation of lactic acid-*
738 *injured Escherichia coli by relieving oxidative stress.* Journal of Applied Microbiology,
739 2019. **127**(6): p. 1741-1750.
740 44. Hohle, T.H. and M.R. O'Brian, *The mntH gene encodes the major Mn(2+) transporter in*
741 *Bradyrhizobium japonicum and is regulated by manganese via the Fur protein.* Mol
742 Microbiol, 2009. **72**(2): p. 399-409.
743 45. Murphy, K.C., S.J. Nelson, S. Nambi, K. Papavinasasundaram, C.E. Baer, and C.M.
744 Sassetti, *ORBIT: a new paradigm for genetic engineering of mycobacterial*
745 *chromosomes.* mBio, 2018. **9**(6): p. e01467-18.
746 46. McBee, M.E., Y.H. Chionh, M.L. Sharaf, P. Ho, M.W.L. Cai, and P.C. Dedon, *Production*
747 *of superoxide in bacteria is stress- and cell state-dependent: A gating-optimized flow*
748 *cytometry method that minimizes ROS measurement artifacts with fluorescent dyes.*
749 Frontiers in Microbiology, 2017. **8**(MAR).

750 47. Wayne, L.G. and L.G. Hayes, *An In Vitro Model for Sequential Study of Shiftdown of*
751 *Mycobacterium tuberculosis through Two Stages of Nonreplicating Persistence.* Infection
752 and Immunity, 1996. **64**(6): p. 2062-2069.
753 48. Brazas Michelle, D., B.M. Breidenstein Elena, J. Overhage, and E.W. Hancock Robert,
754 *Role of Lon, an ATP-Dependent Protease Homolog, in Resistance of Pseudomonas*
755 *aeruginosa to Ciprofloxacin.* Antimicrobial Agents and Chemotherapy, 2007. **51**(12): p.
756 4276-4283.
757 49. Kusser, W. and E.E. Ishiguro, *Involvement of the relA gene in the autolysis of*
758 *Escherichia coli induced by inhibitors of peptidoglycan biosynthesis.* Journal of
759 Bacteriology, 1985. **164**(2): p. 861-865.
760 50. Bokinsky, G., E.E.K. Baidoo, S. Akella, H. Burd, D. Weaver, J. Alonso-Gutierrez, H.
761 García-Martín, T.S. Lee, and J.D. Keasling, *HipA-Triggered Growth Arrest and β-Lactam*
762 *Tolerance in Escherichia coli Are Mediated by RelA-Dependent ppGpp Synthesis.*
763 Journal of Bacteriology, 2013. **195**(14): p. 3173-3182.
764 51. Honsa, E.S., V.S. Cooper, M.N. Mhaissen, M. Frank, J. Shaker, A. Iverson, J. Rubnitz,
765 R.T. Hayden, R.E. Lee, C.O. Rock, E.I. Tuomanen, J. Wolf, and J.W. Rosch, *RelA*
766 *Mutant Enterococcus faecium with Multiantibiotic Tolerance Arising in an*
767 *Immunocompromised Host.* mBio, 2017. **8**(1): p. e02124-16.
768 52. Nguyen, D., A. Joshi-Datar, F. Lepine, E. Bauerle, O. Olakanmi, K. Beer, G. McKay, R.
769 Siehnel, J. Schafhauser, Y. Wang, B.E. Britigan, and P.K. Singh, *Active starvation*
770 *responses mediate antibiotic tolerance in biofilms and nutrient-limited bacteria.* Science,
771 2011. **334**(6058): p. 982-6.
772 53. Kudrin, P., V. Varik, S.R.A. Oliveira, J. Beljantseva, T.D.P. Santos, I. Dzhygyr, D. Rejman,
773 F. Cava, T. Tenson, and V. Hauryliuk, *Subinhibitory Concentrations of Bacteriostatic*
774 *Antibiotics Induce relA-Dependent and relA-Independent Tolerance to*

β-Lactams.* Antimicrobial Agents and Chemotherapy, 2017. **61**(4): p. 10.1128/aac.02173-16.

54. Viducic, D., T. Ono, K. Murakami, H. Susilowati, S. Kayama, K. Hirota, and Y. Miyake, *Functional analysis of spoT, relA and dksA genes on quinolone tolerance in Pseudomonas aeruginosa under nongrowing condition.* Microbiol Immunol, 2006. **50**(4): p. 349-57.

55. Geiger, T., B. Kästle, F.L. Gratani, C. Goerke, and C. Wolz, *Two small (p)ppGpp synthases in Staphylococcus aureus mediate tolerance against cell envelope stress conditions.* J Bacteriol, 2014. **196**(4): p. 894-902.

56. Dutta, N.K., L.G. Klinkenberg, M.J. Vazquez, D. Segura-Carro, G. Colmenarejo, F. Ramon, B. Rodriguez-Miquel, L. Mata-Cantero, E. Porras-De Francisco, Y.M. Chuang, H. Rubin, J.J. Lee, H. Eoh, J.S. Bader, E. Perez-Herran, A. Mendoza-Losana, and P.C. Karakousis, *Inhibiting the stringent response blocks Mycobacterium tuberculosis entry into quiescence and reduces persistence.* Sci Adv, 2019. **5**(3): p. eaav2104.

57. Bhaskar, A., C. De Piano, E. Gelman, J.D. McKinney, and N. Dhar, *Elucidating the role of (p) ppGpp in mycobacterial persistence against antibiotics.* IUBMB life, 2018. **70**(9): p. 836-844.

58. Hunt-Serracín, A.C., M.I. Kazi, J.M. Boll, and C.C. Boutte, *In Mycobacterium abscessus, the Stringent Factor Rel Regulates Metabolism but Is Not the Only (p)ppGpp Synthase.* J Bacteriol, 2022. **204**(2): p. e0043421.

59. Kohanski, M.A., D.J. Dwyer, B. Hayete, C.A. Lawrence, and J.J. Collins, *A common mechanism of cellular death induced by bactericidal antibiotics.* Cell, 2007. **130**(5): p. 797-810.

60. Sebastian, J., S. Swaminath, R.R. Nair, K. Jakkala, A. Pradhan, and P. Ajitkumar, *De Novo Emergence of Genetically Resistant Mutants of Mycobacterium tuberculosis from*

the Persistence Phase Cells Formed against Antituberculosis Drugs In Vitro. Antimicrob Agents Chemother, 2017. **61**(2).

61. Snapper, S.B., L. Lugosi, A. Jekkel, R.E. Melton, T. Kieser, B.R. Bloom, and W.R. Jacobs, Jr., *Lysogeny and transformation in mycobacteria: stable expression of foreign genes.* Proc Natl Acad Sci U S A, 1988. **85**(18): p. 6987-91.

FIGURE 1

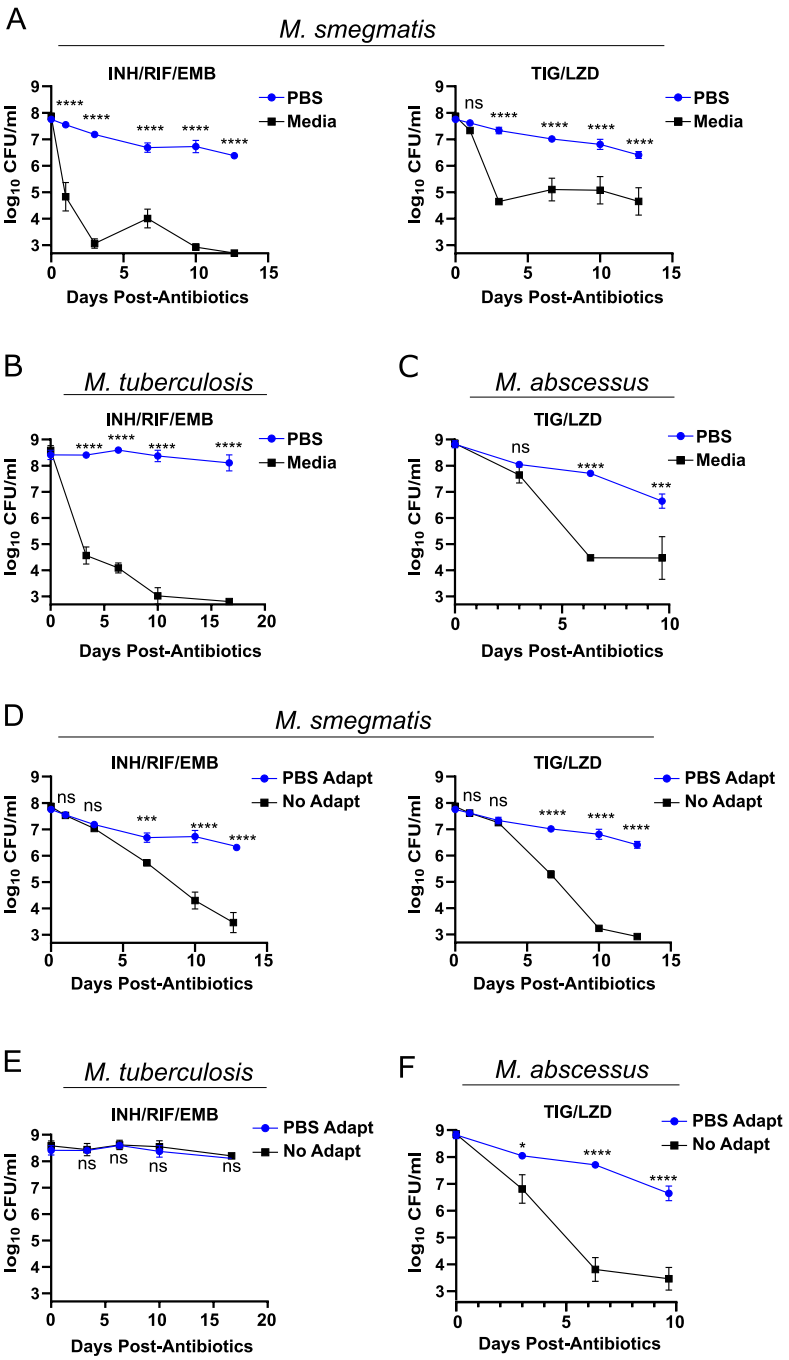

FIGURE 2

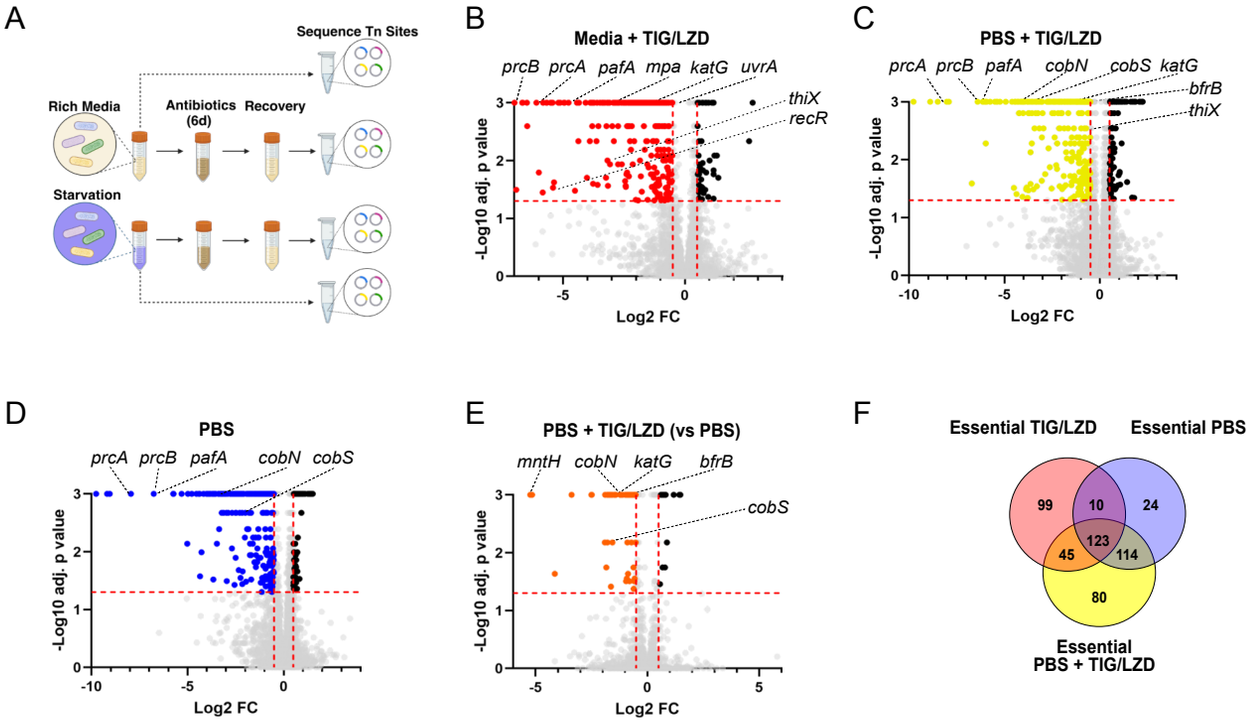

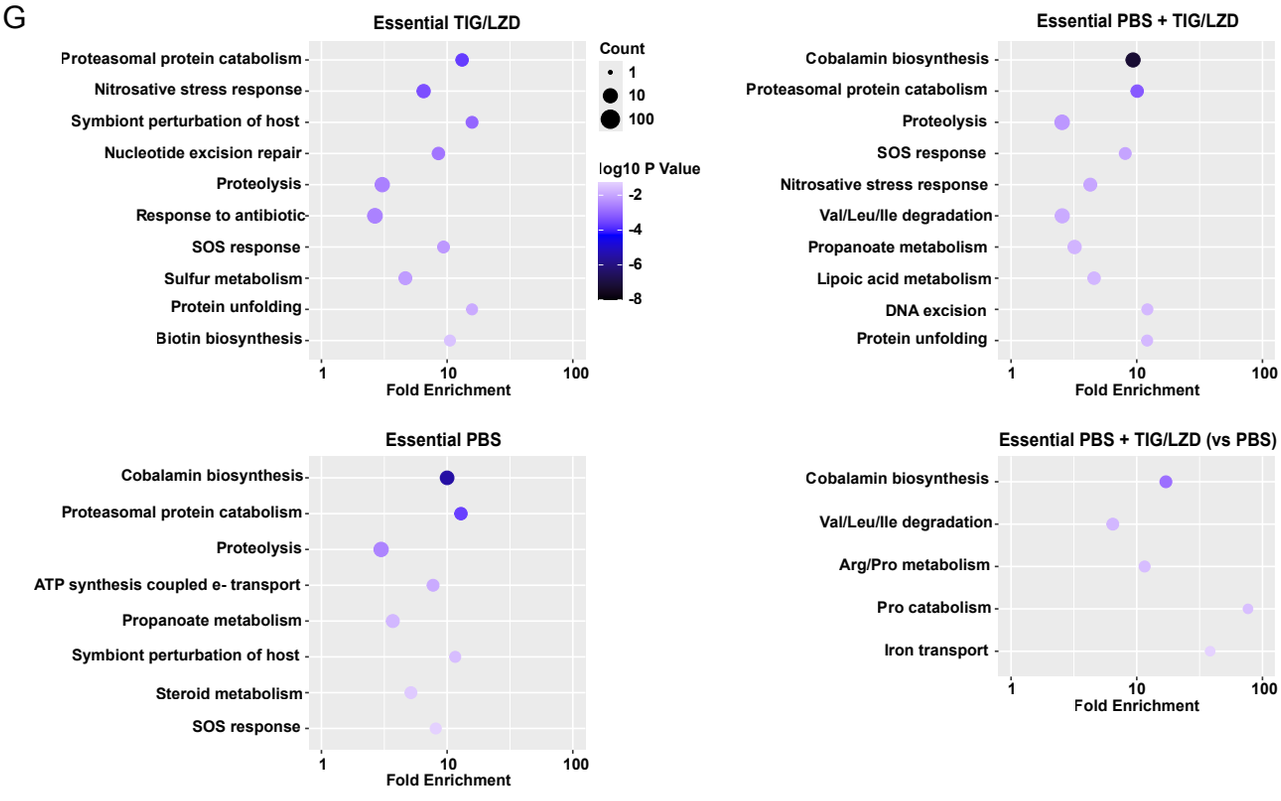

FIGURE 3

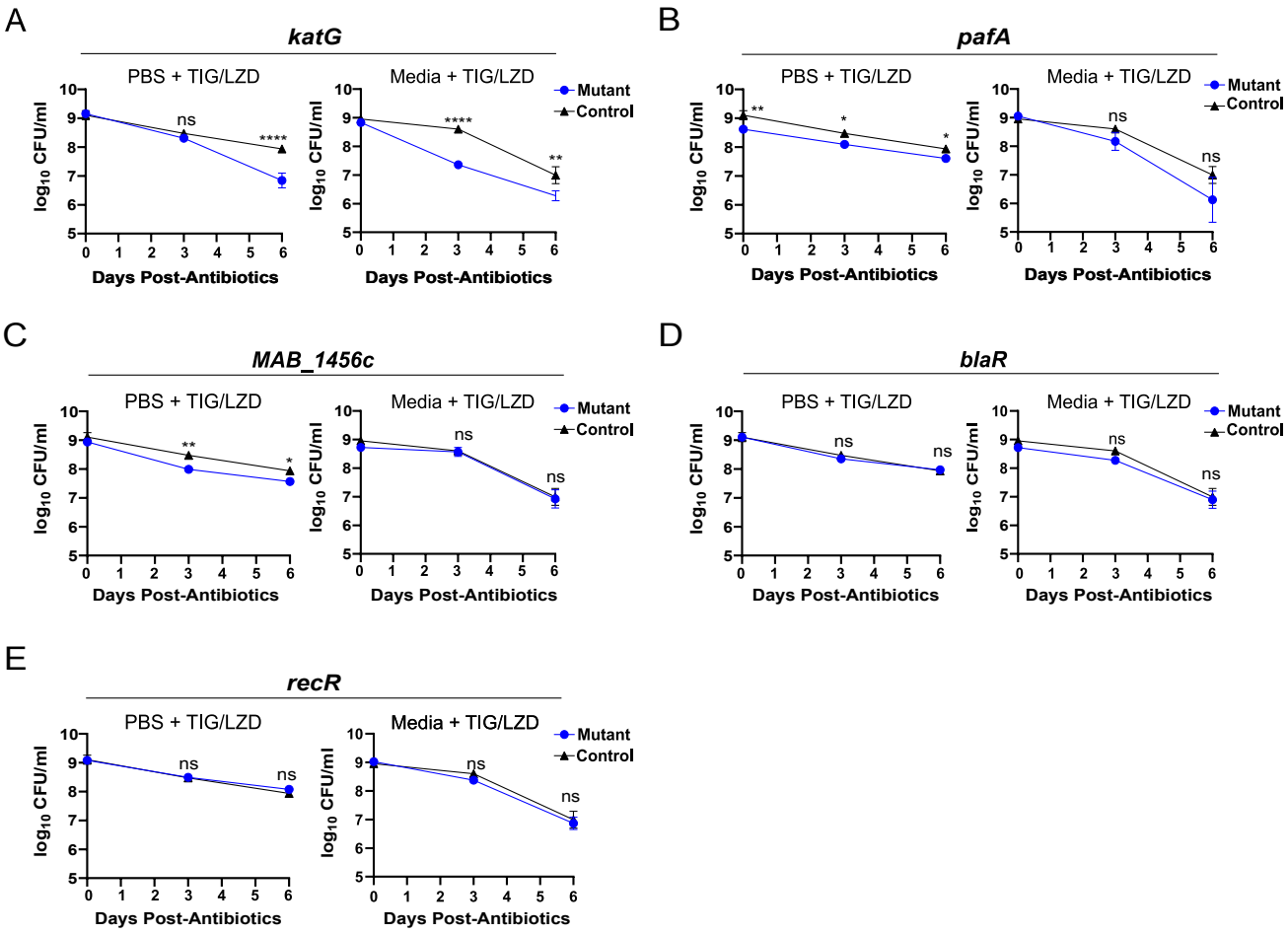

FIGURE 4

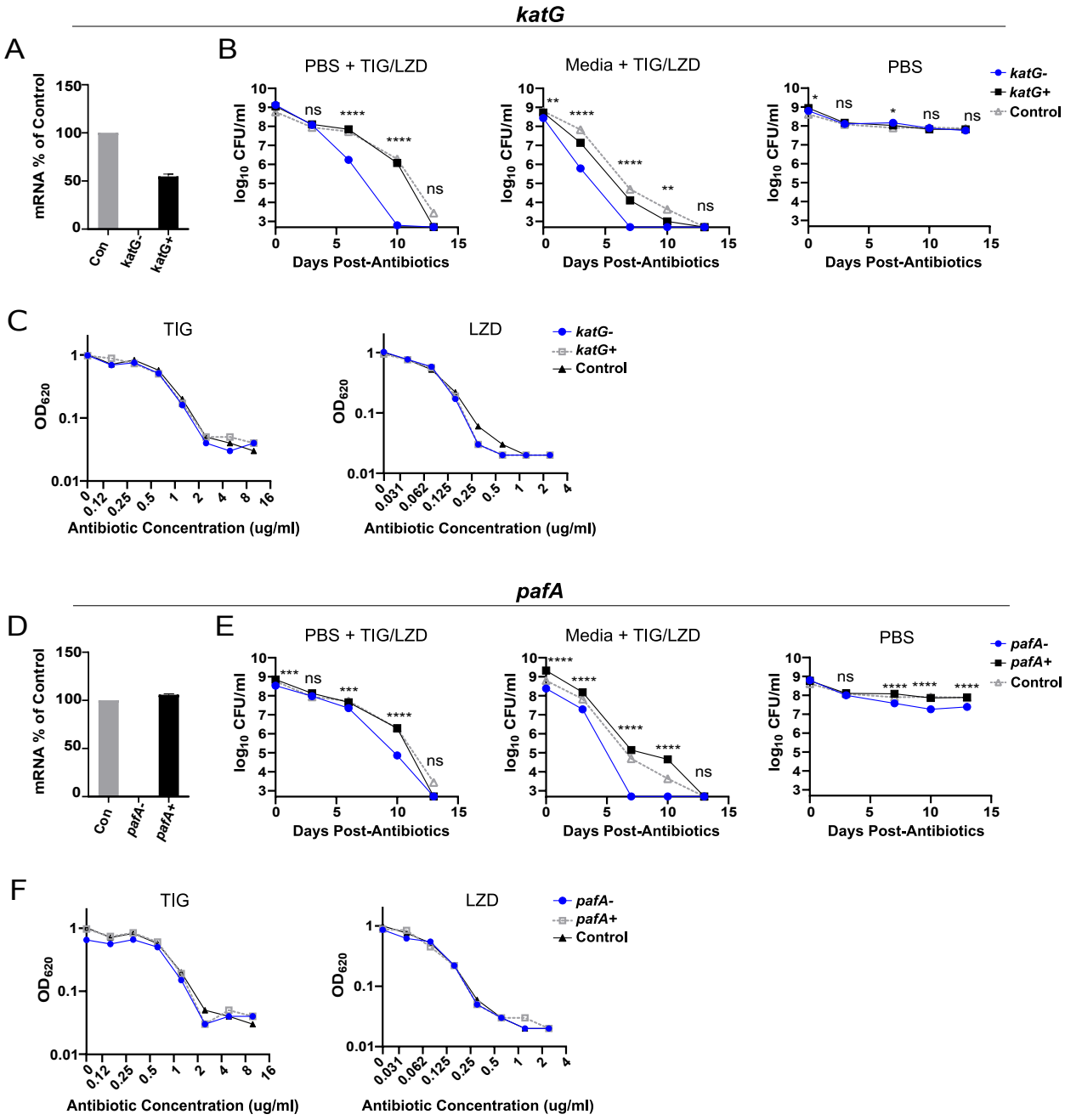

FIGURE 5

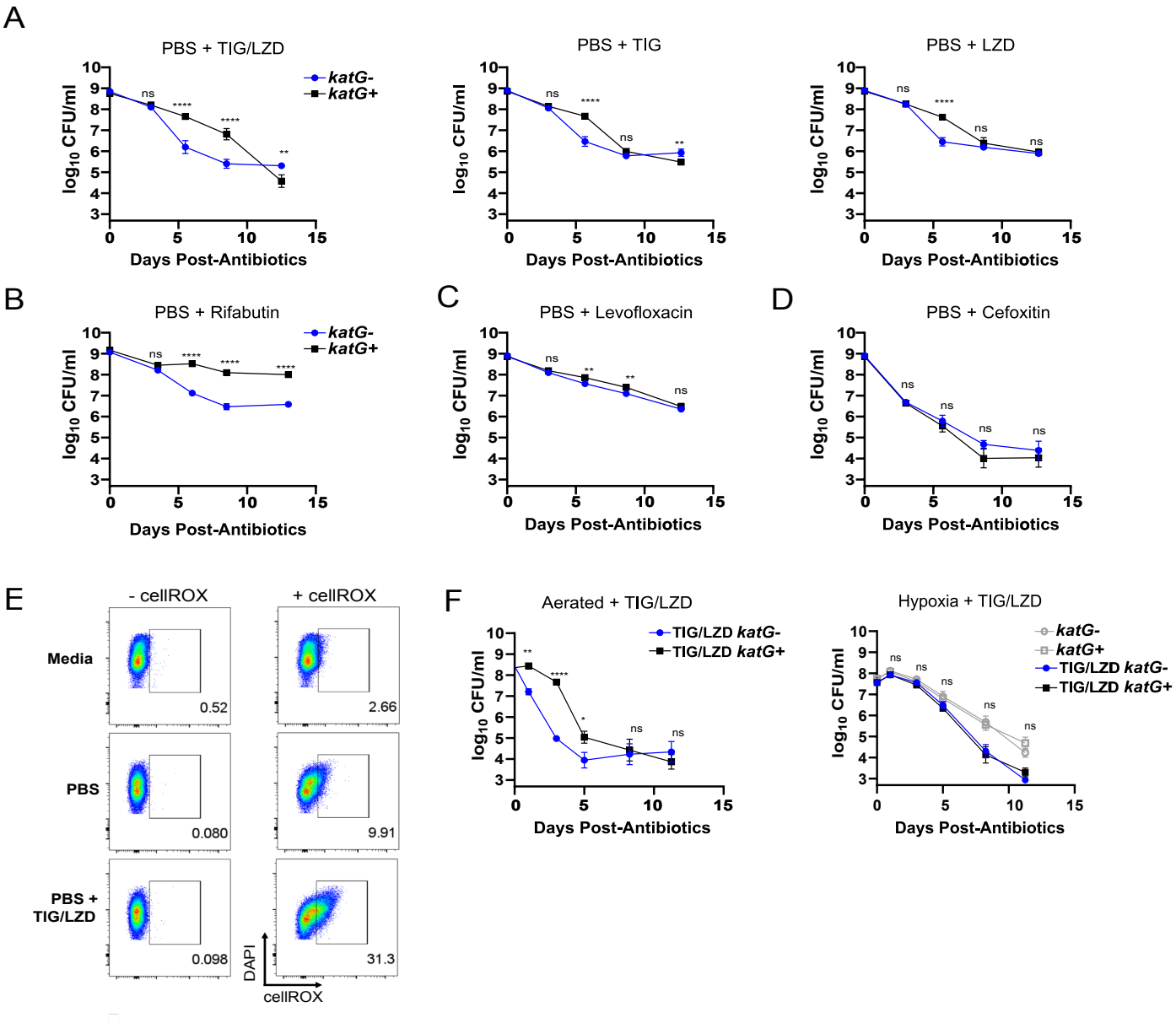

FIGURE 6